We are IntechOpen,
the world's leading publisher of
Open Access books
Built by scientists, for scientists

6,900
Open access books available

185,000
International authors and editors

200M
Downloads

Our authors are among the

154
Countries delivered to

TOP 1%
most cited scientists

12.2%
Contributors from top 500 universities

CLARIVATE ANALYTICS
BOOK CITATION INDEX
INDEXED

WEB OF SCIENCE™

Selection of our books indexed in the Book Citation Index
in Web of Science™ Core Collection (BKCI)

Interested in publishing with us?
Contact book.department@intechopen.com

A Modified Least Mean Square Method Applied to Frequency Relaying

Daniel Barbosa[1], Renato Machado Monaro[2], Ricardo A. S. Fernandes[3],
Denis V. Coury[4] and Mário Oleskovicz[5]

[1]*Salvador University (UNIFACS)*
[2,3,4,5]*Engineering School of São Carlos / University of São Paulo (USP)*
Brazil

1. Introduction

In an Electrical Power System (EPS), a fast and accurate detection of faulty or abnormal situations by the protection system are essential for a faster return to the normal operation condition. With this objective in mind, protective relays constantly monitor the voltage and current signals, including their frequency.

The frequency is an important parameter to be monitored in an EPS due to suffer significant alterations during a fault or undesired situations. In practice, the equipment are designed to work continuously between 98% and 102% of nominal frequency (IEEE Std C37.106, 2004). However, variations on these limits are constantly observed as a consequence of the dynamic unbalance between generation and load. The larger variations may indicate fault situations as well as a system overload. Considering the latter, the frequency relay can help in the load shedding decision and, consequently, in the power system stability. In this way, a prerequisite for stable operation has become more difficult to maintain considering the large expansion of electrical systems (Adanir, 2007; Concordia et al., 1995).

The importance of correct frequency estimation for EPS is then observed, especially if the established limits for its normal operation are not reached. This can cause serious problems for the equipment connected to the power utility, such as capacitor banks, generators and transmission lines, affecting the power balance. Therefore, frequency relays are widely used in the system to detect power oscillations outside the acceptable operation levels of the EPS.

Due to the technological advances and considerable increase in the use of electronic devices of the last decades, the frequency variation analyses in EPS were intensified, since the modern components are more sensitive to this kind of phenomenon.

Taking this into account, the study of new techniques for better and faster power system frequency estimation has become extremely important for a power system operation. Thus, some researchers have proposed different techniques to solve the frequency estimation problem. Algorithms based on the phasor estimation, using the LMS method, the Fast Fourier Transform (FFT), intelligent techniques, the Kalman Filter, the Genetic Algorithms, the Weighted Least Square (WLS) technique, the three-phase Phase-Locked Loop (3PLL) and the Adaptive Notch Filter (Dash et al., 1999; 1997; El-Naggar & Youssed, 2000; Girgis & Ham, 1982; Karimi-Ghartemani et al., 2009; Kusljevic et al., 2010; Mojiri et al., 2010; Phadke et al., 1983; Rawat & Parthasarathy, 2009; Sachdev & Giray, 1985). The adaptive filter based on the

LMS proposed by Pradhan et al. (2005) should be outlined. The LMS was first introduced by Widrow and Hoff (Farhang-Boroujeny, 1999) for digital signal processing and has been widely used because of its simplified structure, efficiency and computing robustness.

In this chapter, will be presented the LMS in its complex form (Widrow et al., 1975) with an adaptive step-size (Aboulnasr & Mayyas, 1997) and some practical aspects of the algorithm implementation, which provides an increased convergence speed. It must be emphasized that the complex signal analyzed is formed by the power system three-phase voltages applying the $\alpha\beta$-Transform (Barbosa et al., 2010).

The algorithm performance was tested by computer simulations using ATP (Alternative Transients Program) software (EEUG, 1987). Some EPS equipment was modelled, including: a synchronous generator with speed governor and voltage control, transmission lines with parameters dependent on the frequency and power transformers. Extreme operational situations were tested in order to observe the behaviour of the proposed technique and validate the obtained results. It must be highlighted that the results of frequency estimation were compared to results of a commercial frequency relay (function 81), and it shows that the adaptive filter theory applied to the digital protection is fast.

2. The algorithm based on LMS

The algorithm based on the LMS method, presented in Fig. 1, is a combination of the adaptive process with digital filtering. In this Figure, $\bar{u}(n-1) = [u(n-1)\ u(n-2)\ ...\ u(n-M)]$ is the vector with M past values of the input $u(n)$; $\bar{w}(n) = [w_1(n)\ w_2(n)\ ...\ w_N(n)]^T$ is the vector with the filter coefficients; $y(n)$ is the desired signal (the output filter) and $e(n)$ is the error associated to the filter approximation.
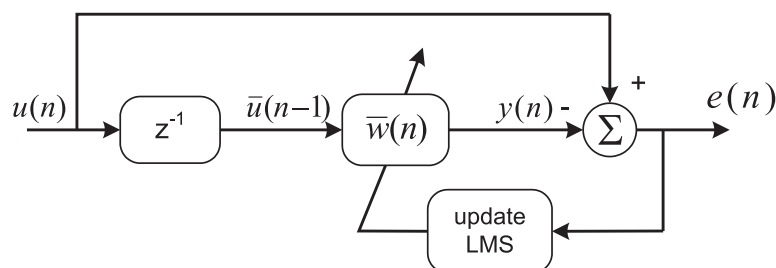

Fig. 1. Adaptive filter based on LMS.

The input signal of the filter can be estimated by minimizing the squared error by the coefficient adaptations ($\bar{w}(n)$), which are recursively adjusted to obtain optimal values. At each iteration, the coefficients can be calculated by:

$$\bar{w}(n+1) = \bar{w}(n) + \mu\left(-\nabla(n)\right),\qquad(1)$$

where μ is the convergence parameter and ∇ is the gradient of error performance surface and is responsible for determining the adjustment of coefficients.

The LMS algorithm is very sensitive to μ. This can be mainly observed by the speed of the estimation and processing time. The lesser μ value, the longer the time to reach the aimed error and vice-versa. However, it is important to respect the convergence interval given by (Haykin, 2001):

$$0 < \mu < \frac{1}{NS_{max}},\qquad(2)$$

where N is the filter size and S_{max} is the maximum power spectral density value of the input signal.

3. The adaptive algorithm and the frequency estimation

The study of digital filters is a consolidated research area. Regarding digital protection, digital filters provide the frequency component extraction used in digital relay algorithms. The information contained in the input data from a three-phase system can be processed simultaneously, making it possible to obtain more precise results if compared to conventional methods.

It must be highlighted that the proposed algorithm, called Frequency Estimation Algorithm by the Least Mean Square (FEALMS), uses three-phase signals as inputs. It is considered that the three-phase voltages from EPS can be represented by:

$$
\begin{aligned}
V_a(n) &= A_{max}cos(\omega n\Delta t + \phi) + \xi_{n_a} \\
V_b(n) &= A_{max}cos(\omega n\Delta t + \phi - \tfrac{2\pi}{3}) + \xi_{n_b}, \\
V_c(n) &= A_{max}cos(\omega n\Delta t + \phi + \tfrac{2\pi}{3}) + \xi_{n_c}
\end{aligned}
\tag{3}
$$

where, A_{max} is the peak value; ω is the signal angular frequency [1]; n is the sample number of the discrete signal; Δt is the time between two consecutive samples; ϕ is the signal phase and ξ_n is the error between two consecutive samples. Fig. 2 illustrates the proposed relay algorithm.
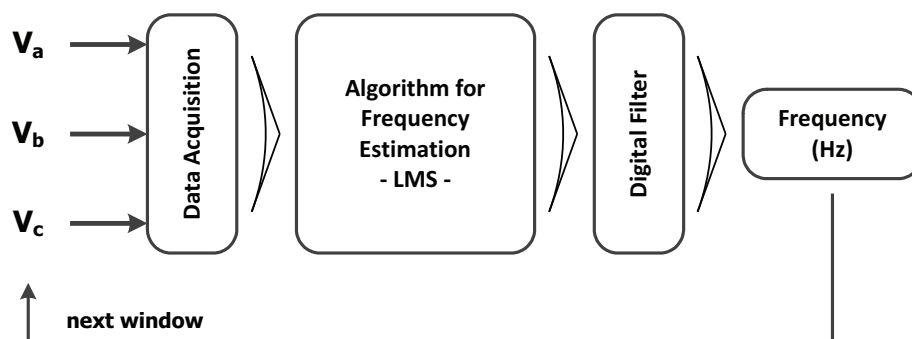

Fig. 2. Basic relay algorithm.

3.1 The data acquisition

All the stages in data acquisition are performed with the aim of having a more realistic analysis of the obtained results. The input voltage signals simulated are characterized by a high sampling rate in order to represent the analog signals more realistically.

A flowchart that represents the procedure of data acquisition can be visualized by means of Fig. 3. A second order Butterworth low pass filter with a cut–off frequency of $200Hz$ was utilized. A sample rate of $1,920Hz$ and an analog–to–digital converter (ADC) of 16 bits were also used.

The low pass filter was used to avoid spectral spreading and to make sure that the digital representation after ADC conversion is a good representation of the original signal. It is worth commenting that a low cut–off frequency of $200Hz$ was used in order to stabilise the method and ensure that the LMS algorithm will converge. Due to this situation, most of the harmonic components were eliminated, increasing the precision of the proposed method.

[1] $\omega = 2\pi f$, where f is the fundamental frequency of the electrical system
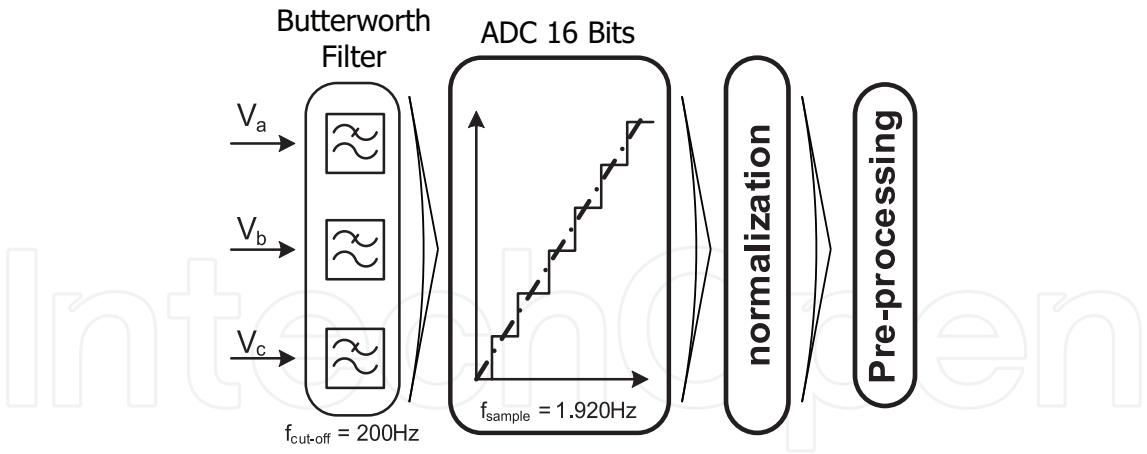
Fig. 3. Data acquisition flowchart.

The data acquisition was performed in a moving window with one sample step. All the filter processing should be performed on one data window, respecting the available time for processing, which is the time between two consecutive samples. Fig. 4 illustrates this process.
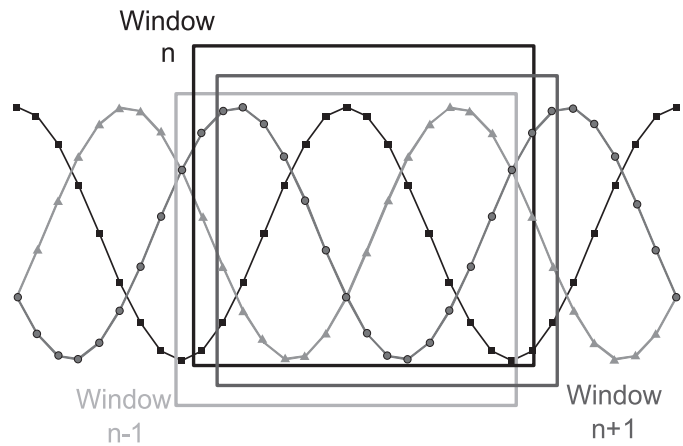

Fig. 4. Moving window process.

3.2 The normalization process
Normalization standardises the data obtained from the electrical system, regardless of the voltage level analysed. Consequently, if either a sag or a swell occurs in any phase, the algorithm will maintain its estimation without loss of precision or speed. Fig. 5 illustrates the normalisation process implemented.

3.3 The pre-processing process
After normalisation, a pre-processing stage was performed, obtaining the signal in its complex form for the digital filter. This was obtained by applying the $\alpha\beta$–Transform on the three-phase voltages, as represented in the following equation (Akke, 1997):

$$\begin{bmatrix} V_\alpha(n) \\ V_\beta(n) \end{bmatrix} = \sqrt{\frac{2}{3}} \begin{bmatrix} 1 & -\frac{1}{2} & -\frac{1}{2} \\ 0 & \frac{\sqrt{3}}{2} & -\frac{\sqrt{3}}{2} \end{bmatrix} [V(n)], \tag{4}$$

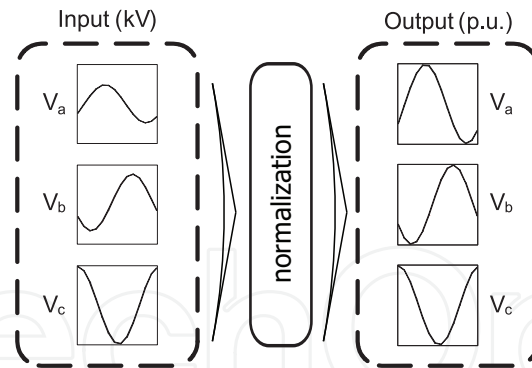where $V(n) = \begin{bmatrix} V_a(n) & V_b(n) & V_c(n) \end{bmatrix}^T$.

Fig. 5. Data normalization flowchart.

After the pre-processing stage, in order to obtain the α and β components by (4), the complex voltage is defined as:

$$u(n) = V_\alpha(n) + jV_\beta(n). \tag{5}$$

3.4 The coefficient generator

Adapting the filter coefficients is simple and inherent to the algorithm. This adjustment is performed sample by sample in order to make sure that the squared average error is minimised. However, to improve the algorithm performance and minimise the processing time, the estimation filter coefficients ($\bar{w}(n)$) are initialised with the estimation of the previous window (Barbosa et al., 2010). The first window is initialised with the fundamental frequency of the electrical system. The aim of this procedure is to increase the speed of the estimation process. The coefficient generator flowchart is shown in Fig. 6.
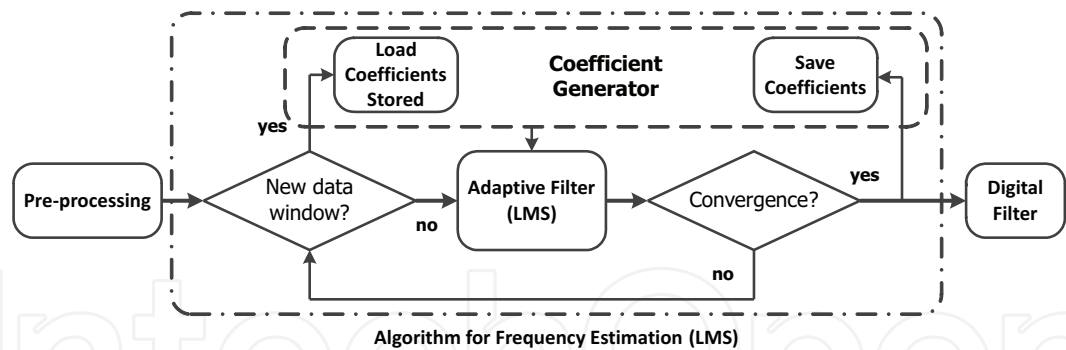

Fig. 6. Coefficient generator flowchart.

3.5 The adaptive filter

In the adaptive filter, the coefficients are updated recursively to minimise the squared error. The error is calculated as the difference between desired and estimated values, given by:

$$e(n) = u(n) - y(n), \tag{6}$$

where $y(n)$ represents the estimated value. The complex voltage ($u(n)$) can be described by:

$$\begin{aligned} u(n) &= U_{max}e^{j(\omega n\Delta T + \phi)} + \zeta(n) \\ &= y(n) + \zeta(n), \end{aligned} \tag{7}$$

where U_{max} is the amplitude of the complex signal, ζ is the noise component, ΔT is the sampling interval, ϕ is the phase of signal, n is the sample number and ω is the angular frequency of the analyzed signal. The estimated complex voltage ($y(n)$) can be represented by equation (8).

$$y(n) = y(n-1)e^{j\omega\Delta T}. \tag{8}$$

The equations (8) and (7) are the base of used model for proposed frequency estimation. Although the output filter can be represented by previous model, it is a linear combination between the input vector, lagged by one sample, and the vector with filter coefficients as illustrated below.

$$y(n) = \bar{w}^H(n)\bar{u}(n-1), \tag{9}$$

where H is the Hilbert transform and $\bar{w}$ is the vector with filter coefficients. This vector denotes the difference between two consecutive samples, ie, the phase difference between the samples being analyzed, according to the equation (10).

$$\bar{w}(n) = e^{j\bar{\omega}(n-1)\Delta T}, \tag{10}$$

where, $\bar{\omega}$ is the estimated angular frequency.

It must be emphasised that the LMS task is to find the filter coefficients that minimize the error. Following this procedure, the filter coefficients are updated until the error is sufficiently small. The complex weight vector at each sampling instant is given by (Widrow et al., 1975):

$$\bar{w}(n+1) = \bar{w}(n) + \mu(n)e(n)^*\bar{u}(n-1), \tag{11}$$

where the ($*$) symbol denotes the complex conjugate and μ is the convergence factor controlling the stability and rate of convergence of the algorithm. Fig. 7 shows the evolution of the adaptive filter coefficients of eighth order during the iterations.

a) Real part.   b) Imaginary part.
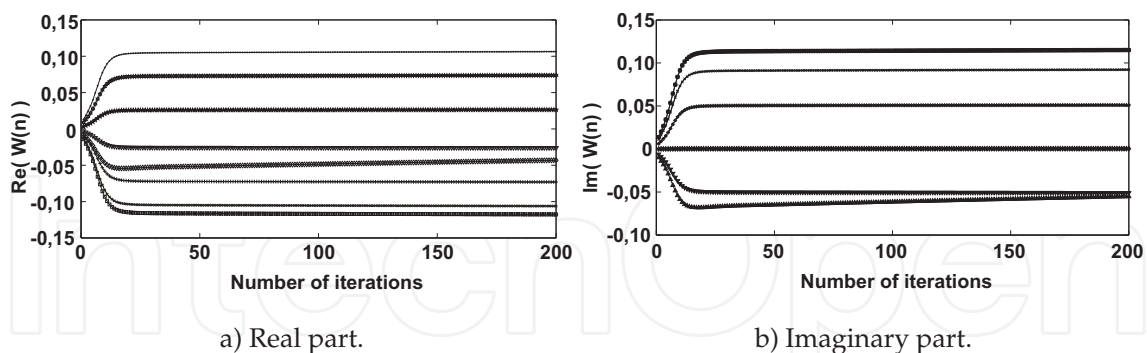
Fig. 7. The adaptive filter coefficient update.

The step size $\mu(n)$ is modified for better convergence in the presence of noise and its equation is given by (Aboulnasr & Mayyas, 1997):

$$\mu(n+1) = \lambda\mu(n) + \gamma p(n)p(n)^*, \tag{12}$$

where $p(n)$ represents the autocorrelation error and it is calculated as:

$$p(n) = \rho p(n-1) + (1-\rho)e(n)e(n-1). \tag{13}$$

In the equation, ρ is the exponential weighting parameter. The ρ $(0 < \rho < 1)$, λ $(0 < \lambda < 1)$ and γ $(0 < \gamma)$ are constants that control the convergence time and they are determined by statistical studies (Kwong & Johnston, 1992).

3.6 The stability of the proposed algorithm

The stability is a critical factor in proposed algorithm implementation, especially if the convergence factor (μ) is out of range associated. Due to these problems, a continuous monitoring of data window samples is performed, providing a self-tuning range of convergence. The behavior of μ is controlled by equation (14) (Wies et al., 2004):

$$0 < \mu < \frac{1}{\frac{N}{M} \sum_{n=0}^{M-1} u(n)u(n)^*}, \tag{14}$$

where N and M are the filter and window sizes, respectively. Fig. 8 shows the proposed algorithm flowchart with the stability control.
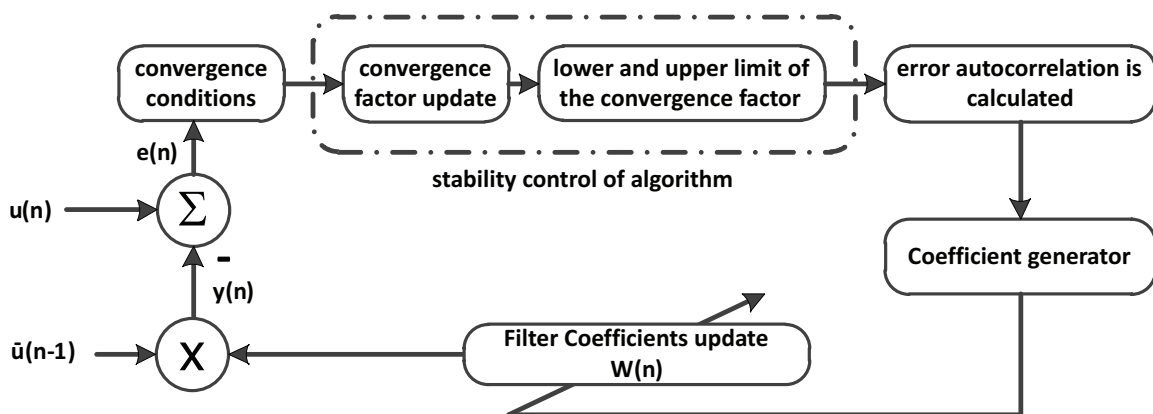

Fig. 8. Proposed algorithm flowchart.

3.7 The frequency estimation

The frequency estimation was performed according to Begovic et al. (1993). To find the phase difference, the complex variable Γ was defined as:

$$\Gamma = y(n)y(n-1)^*. \tag{15}$$

The relationship between Γ and the system frequency is obtained by equation expansion above. This expanding is shown by:

$$\begin{aligned}
\Gamma &= U_{max}^2 \left[e^{j(\omega n \Delta T + \phi)} e^{-j(\omega(n-1)\Delta T + \phi)} \right] \\
&= U_{max}^2 \left[e^{j(\omega n \Delta T + \phi - \omega n \Delta T + \omega \Delta T - \phi)} \right] \\
&= U_{max}^2 e^{j2\pi f_{est}\Delta T} \\
&= U_{max}^2 \left\{ cos(2\pi f_{est}\Delta T) + j sin(2\pi f_{est}\Delta T) \right\},
\end{aligned} \tag{16}$$

where $U_{max} = 1$, once the input signal is normalized, and f_{est} is the estimated frequency. The frequency of the estimated signal $(y(n))$ was calculated in function of the phase difference between two consecutive samples, and the latter was provided by the equation below:

$$f_{est} = \frac{f_s}{2\pi} \arctan\left(\frac{\Im(\Gamma)}{\Re(\Gamma)}\right), \tag{17}$$

where f_s is the sampling frequency and $\Re()$ and $\Im()$ are the real and imaginary parts, respectively.

3.8 The convergence process

The stop rule adopted was the maximum number of iterations (1,000) or error smaller than 10^{-5}. This error can be estimated by:

$$e_{relat} = abs\left(y(n) - u(n)\right), \tag{18}$$

where e_{relat} is the relative error between samples, $abs()$ is the absolute value, $y(n)$ is the estimated value and $u(n)$ is the desired value or input sample.

3.9 The post-processing process of the output signal

The output signal (estimated frequency) is additionally filtered by a second order Butterworth low pass digital filter with a cut–off frequency of $5Hz$. This procedure reduces the oscillation present in the proposed method output, avoiding errors due to abrupt variations of the frequency. It is important to observe that the delay of the low pass filter does not influence the algorithm performance negatively as can be seen in the results.

4. The power system simulation

Fig. 9 shows the representation of the simulated electrical system, taking into account load switching and permanent faults in order to evaluate the frequency estimation technique proposed in this work.
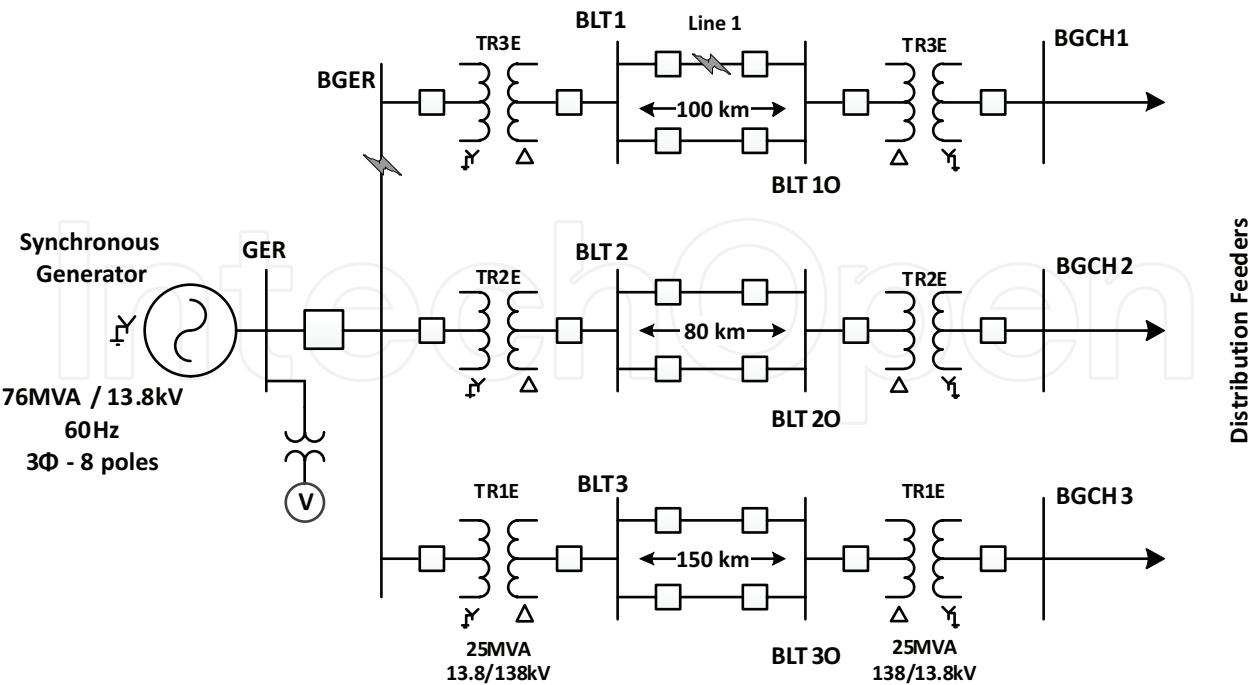

Fig. 9. The power system representation using ATP software.

The electrical system consists of a 13.8 kV and 76 MVA (60Hz) synchronous generator, 13.8:138 kV /138:13.8 kV and 25 MVA three phase power transformers, transmission lines between 80 and 150 km in length and loads between 5 and 25 MVA with a 0.92 inductive power factor. Power transformers have a delta connection in the high voltage winding and a star connection in the low voltage winding. The power transformers were modeled using ATP software (saturable transformer component) considering their saturation curves as illustrated in Fig. 10. Tables 1 and 2 show the parameters used in order to simulate the power system components using ATP software.
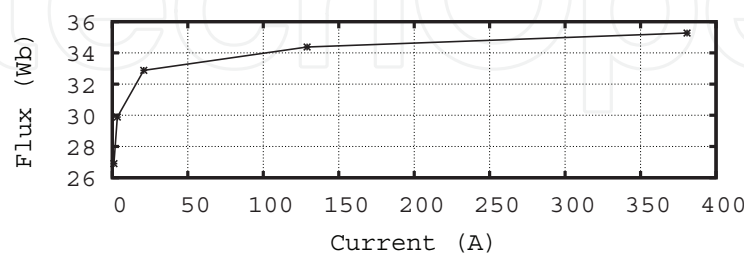

Fig. 10. Saturation curve of power transformers.

Description	Value (unit)	Description	Value (unit)
S	76 (MVA)	N_p	8
V_L	13.8 (kV$_{rms}$)	f	60 (Hz)
I_{FD}	250 (A)	R_a	0.004 (p.u.)
X_l	0.175 (p.u.)	X_o	0.132 (p.u.)
X_d	1.150 (p.u.)	X_q	0.685 (p.u.)
X'_d	0.310 (p.u.)	X''_d	0.210 (p.u.)
X''_q	0.182 (p.u.)	τ'_{do}	5.850 (sec)
τ''_{do}	0.036 (sec)	τ''_{qo}	0.073 (sec)

Table 1. Synchronous generator data used in the simulation.

In Table 1, S is the total three-phase volt-ampere rating of the machine, N_p is the number of poles which characterise the machine rotor, V_L is the rated line-to-line voltage of the machine, f is the electrical frequency of generator, I_{FD} is the field current, R_a is the armature resistance, X_l is the armature leakage reactance, X_o is the zero-sequence reactance, X_d is the direct-axis synchronous reactance, X_q is the quadrature-axis synchronous reactance, X'_d is the direct-axis transient reactance, X''_d is the direct-axis subtransient reactance, X''_q is the quadrature-axis subtransient reactance, τ'_{do} is the direct-axis open-circuit transient time constant, τ''_{do} is the direct-axis open-circuit subtransient time constant and τ'_{qo} is the quadrature-axis open-circuit transient time constant.

Element	$R_+(\Omega)$	$L_+(mH)$
Primary impedance of transformer	1.7462	151.37
Secondary impedance of transformer	0.0175	1.514

Table 2. Power Transformer data used in the simulation.

It is important to emphasise that the transmission line model used was JMARTI from ATP. This was because it is possible to have a variation of the line parameters in function of the frequency and consequently obtain a better representation of the system's behavior when facing disturbances resulting from unbalance between generation and load.

It must also be emphasised that the synchronous generator was simulated with an automatic speed control for hydraulic systems (Boldea, 2006) and automatic voltage regulation (AVR) (Boldea, 2006; Lee, 1992; Mukherjee & Ghoshal, 2007), considering various electrical and mechanical parameters from the generator. Equation 19 shows the transfer function of the speed regulator used:

$$\frac{\eta(s)}{\Delta F(s)} = -\frac{1}{R} \cdot \frac{1 + sT_r}{\left(1 + sT_g\right)\left(1 + s\frac{r}{R}T_r\right)} \tag{19}$$

where $\eta(s)$ is the servomotor position, $\Delta F(s)$ is the frequency deviation, R is the steady-state speed droop, r is the transient speed droop, T_g is the main gate servomotor time constant and T_r is the reset time. Table 3 presents the parameters concerning the speed regulator.

Description	Value (unit)
Main gate servomotor time constant (T_g)	0.600 (sec)
Reset time (T_r)	0.838 (sec)
Transient speed droop (r)	0.279
Steady-state speed droop (R)	0.100
Moment of inertia (M)	1.344 (sec)
Water starting constant (T_W)	0.150 (sec)

Table 3. Parameters concerning the speed regulator.

Fig. 11 shows the block diagram of the excitation control system which was used. The basic function of the excitation control system automatically adjusts the magnitude of the DC field current of the synchronous generator to maintain the terminal voltage constant as the output varies according to the capacity of the generator (Kundur, 1994).
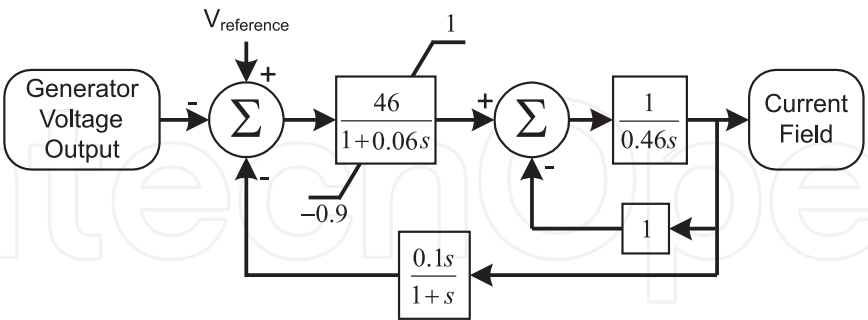

Fig. 11. Block diagram of the excitation control system.

The field voltage control can improve the transient stability of the power system after a major disturbance. However, the extent of the field voltage output is limited by the exciter's ceiling voltage, which is restricted by generator rotor insulation (Kundur, 1994; Leung et al., 2005).

5. Test cases

This section presents results of the proposed scheme. Although a great deal of data was used to test the proposed technique, only four cases of abnormal operation were carefully chosen to

illustrate the technique performance concerning the electrical system presented in Fig. 9. Each condition imposes a particular dynamic behavior in the power balance and, consequently, in the variation of the power system frequency. Measurements from a commercial relay (function 81) were obtained by using the simulated voltage signals from ATP in order to compare the results. Moreover, the actual frequency of the EPS was measured directly from the angular speed of the synchronous generator. It should be emphasized that the sample rates of $1,920Hz$ and $1,000Hz$ were used in the FEALMS software and a commercial relay (function 81), respectively.

Due to a great influence from the adjustment of the filter parameters in the results, these parameters were selected according to Kwong & Johnston (1992), and they are: $\mu_{max} = 0.18$, $\mu_{min} = 0.001$, $p_{inicial} = 0$, $\lambda = 0.97$, $\gamma = 0.01$ and $\rho = 0.99$. Based on Fig. 9, the simulated situations were:

- a sudden connection of load blocks;

- a permanent fault involving phase A and ground (AG) on the BGER busbar at 2s;

- a sudden disconnection of TR1E and TR3E transformers at 1s;

- a permanent fault at 50% of line 1;

- the generator overexcitation;

- the TR3E transformer energization with full load.

5.1 A sudden connection of load blocks

Fig. 12(a) shows the estimation of the synchronous generator frequency using the FEALMS, the ATP software reference curve and the commercial frequency relay responses considering the connection of load blocks in the BGCH3 busbar. In the figure, a slight delay in the frequency estimation by the relay can be observed, when compared to the correct result given by the ATP software curve. In this situation, a very good precision concerning the FEALMS can be observed, even in critical points of the system's behavior. The error concerning the application of the proposed technique is also presented as illustrated in Fig. 12(b).
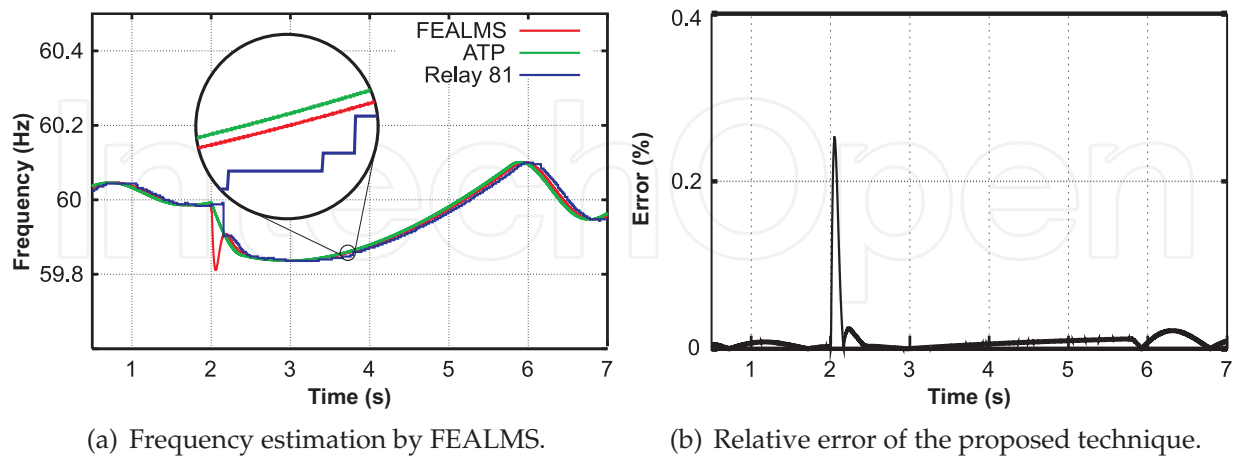

(a) Frequency estimation by FEALMS. (b) Relative error of the proposed technique.

Fig. 12. Connection of load blocks on the BGCH3 busbar at 2s.

5.2 A permanent fault involving phase A and ground (AG) on the BGER busbar at 2s

Fig. 13(a) shows the estimation given by the proposed technique, the ATP reference curve, as well as the commercial frequency relay performances for an AG fault on the BGER busbar at 2s.
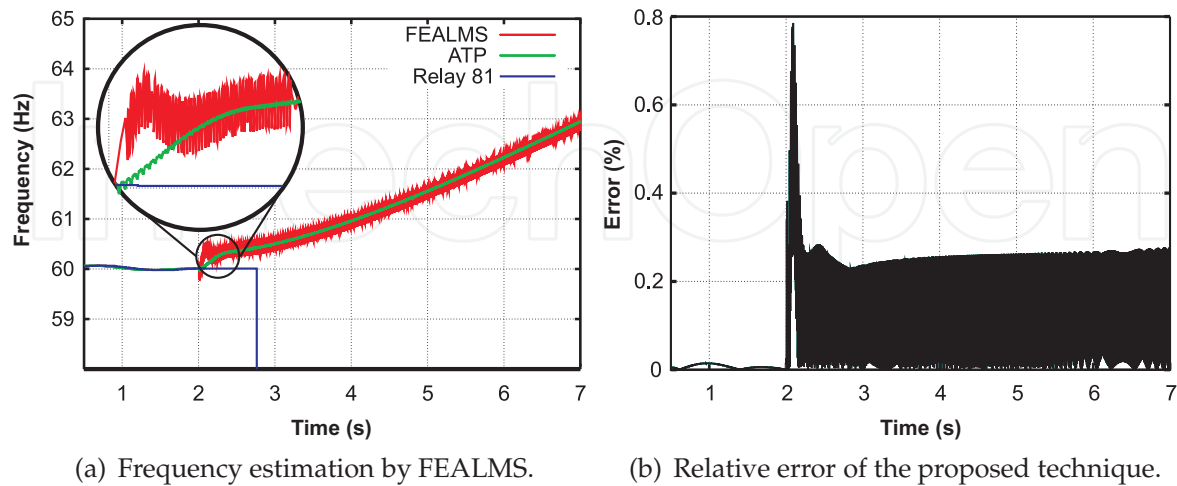

(a) Frequency estimation by FEALMS.   (b) Relative error of the proposed technique.

Fig. 13. AG fault on BGER busbar at 2s.

It can be seen that the commercial frequency relay tested loses the reference voltage, hindering the frequency estimation. It should be emphasized that even in this unfavorable condition, the FEALMS estimated the power system frequency satisfactorily.

5.3 A sudden disconnection of TR1E and TR3E transformers at 1s

Fig. 14(a) also illustrates the FEALMS responses, the ATP reference curve, as well as the commercial frequency relay for a disconnection of TR1E and TR3E transformers. The analysis of this condition is fundamental to test the algorithm's robustness facing practical field situations, taking into account the high level of distortion presented in the input signals.

(a) Frequency estimation by FEALMS.   (b) Relative error of the proposed technique.
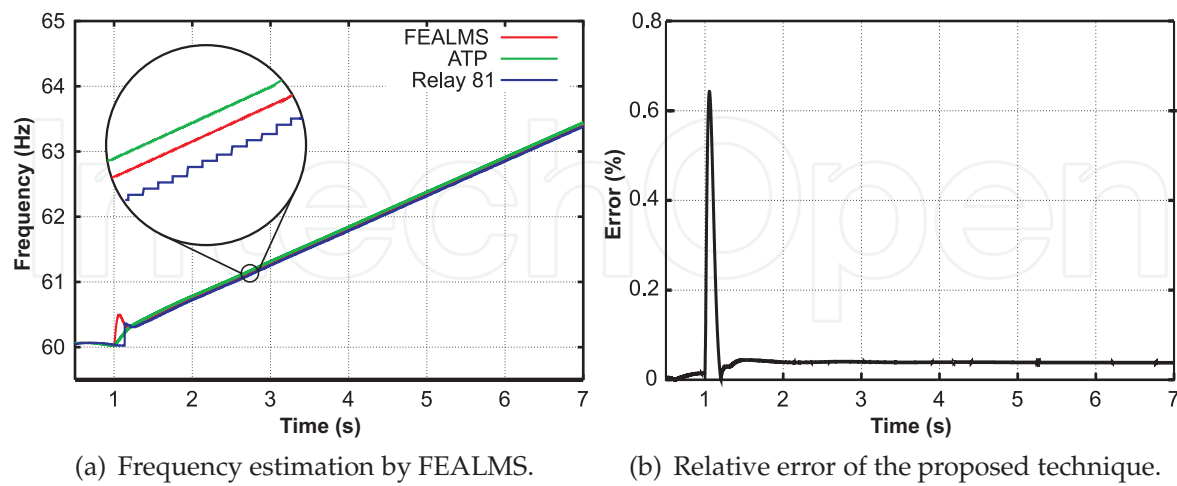
Fig. 14. A sudden disconnection of TR1E and TR3E transformers at 1s.

It can be clearly observed that the commercial relay (function 81), as well as the FEALMS, presented similar satisfactory responses. Once more, a delay can be observed for the commercial relay (function 81), possibly due to the filtering process.

5.4 A permanent fault at 50% of line 1

In Fig. 15, a frequency variation and relative error of frequency estimation by the proposed technique are observed considering an AG fault at 50% of the transmission length of line 1. In this situation, the correspondent three-phase circuit breaker opened after 80ms from the fault inception.
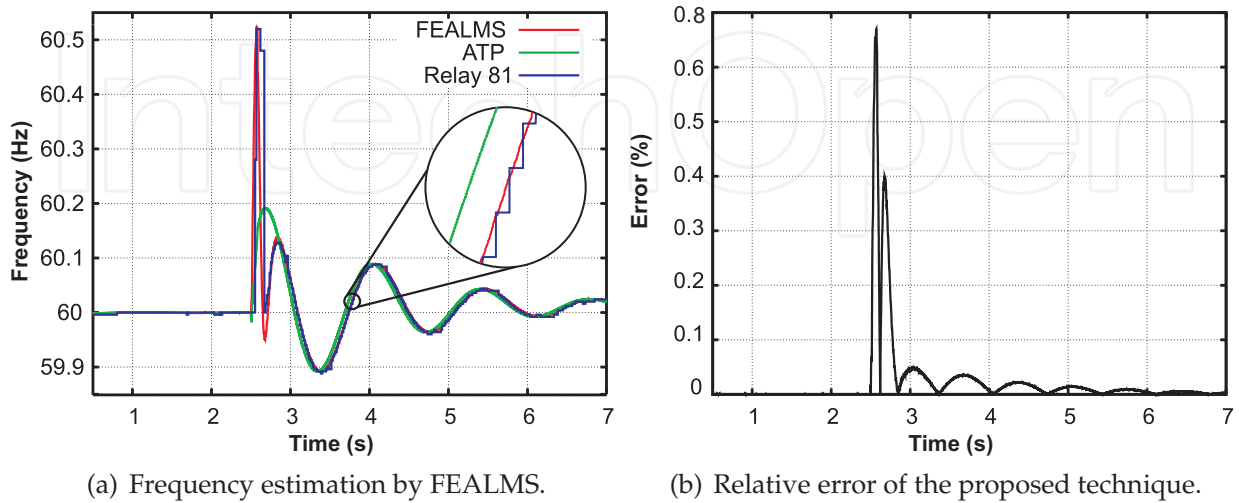

(a) Frequency estimation by FEALMS.   (b) Relative error of the proposed technique.

Fig. 15. AG fault at 50% of the line 1 length.

It should also be observed that the recovery of the machine synchronization was achieved in this situation.

5.5 The generator overexcitation

Fig. 16(a) illustrates the FEALMS and commercial relay (function 81) responses, as well as the ATP reference curve for the generator overexcitation. This situation illustrates the ability of the algorithm to estimate the frequency in the presence of harmonics in the input signals.
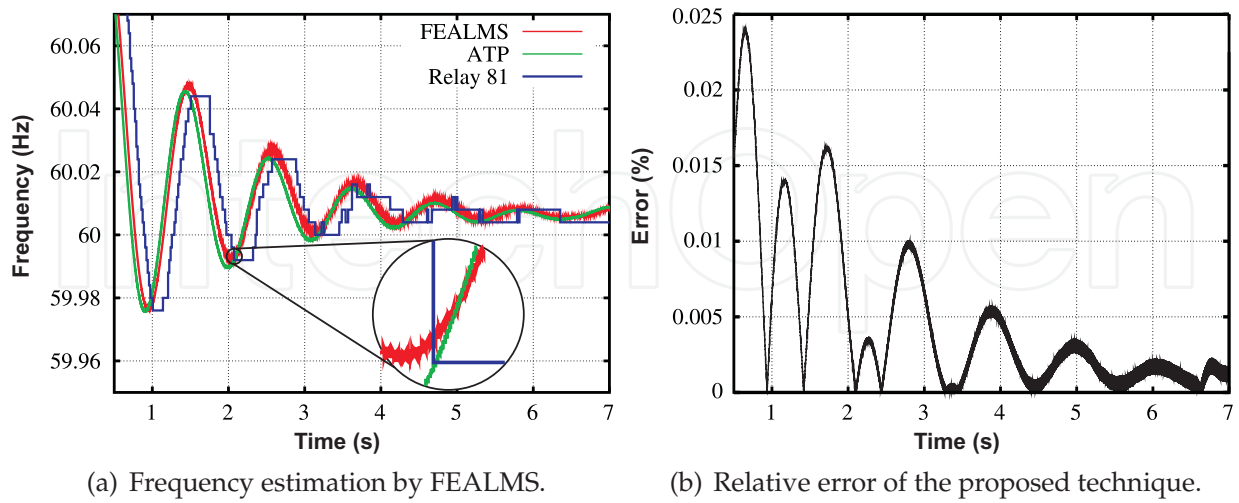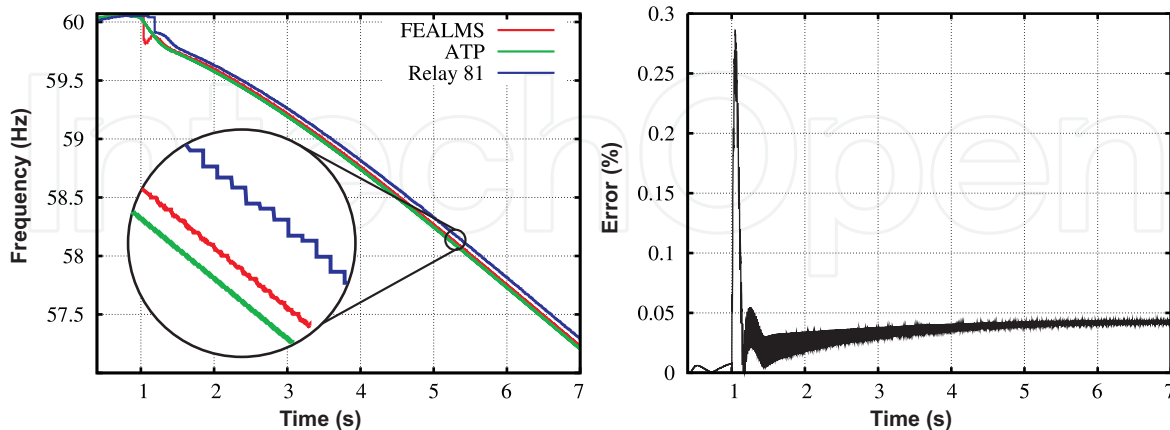

(a) Frequency estimation by FEALMS.   (b) Relative error of the proposed technique.

Fig. 16. Frequency estimation for generator overexcitation.

5.6 The TR3E transformer energization with full load

Fig. 17(a) illustrates the frequency estimation of the proposed technique together with the commercial frequency relay performance, as well as the ATP reference curve for a case of frequency drop concerning TR3E transformer energization with full load.

(a) Frequency estimation by FEALMS.   (b) Relative error of the proposed technique.

Fig. 17. TR3E transformer energization with full load.

It can be seen from Fig. 17(b) that most of the estimation errors for FEALMS are below 0.05%.

6. Conclusions

This chapter presented an alternative method for the frequency estimation in electrical power systems using the modified LMS algorithm. The implementation of digital filtering and the $\alpha\beta$–Transform in the proposed technique made the simultaneous use of the three-phase power system voltages for the estimation purpose possible.

In the complex LMS algorithm considered, the adjustment of the step size was used as being adaptive based on the estimations of the error.

The simulations used for testing the proposed algorithm were obtained using ATP software. The adaptive filter theory applied to the digital protection was fast and reliable. Some points should be observed:

1. The FEALMS algorithm can be applied to various situations and voltage levels, as it is not influenced by the magnitude of the input waveforms;

2. Three-phase voltages were analysed contrary to a single phase (used in commercial relays), making the proposed algorithm more robust;

3. The technique is easy to implement and does not need adjustments and knowledge of further functions, as is the case of the commercial relay (function 81) which was used;

4. Applying FEALMS algorithm, the average error in all cases studied was 0.08%.

It is also important to highlight the feasibility and computing efficiency of this method, make it suitable for commercial applications.

7. References

Aboulnasr, T. & Mayyas, K. (1997). A robust variable step-size LMS-type algorithm: Analysis and simulations, *IEEE Transactions on Signal Processing* 45(3): 631–639.

Adanir, T. (2007). Extremely short term frequency estimation (estfe) algorithm for underfrequency protection, *International Journal of Electrical Power & Energy Systems* 29(4): 329–337.

Akke, M. (1997). Frequency estimation by demodulation of two complex signals, *IEEE Transactions on Power Delivery* 12(1): 157–163.

Barbosa, D., Monaro, R. M., Coury, D. V. & Oleskovicz, M. (2010). Digital frequency relaying based on the modified least mean square method, *International Journal of Electrical Power & Energy Systems* 32(3): 236 – 242.
URL: *http://www.sciencedirect.com/science/article/B6V2T-4X076Y8-2/2/fe189bb77b1dd0 aedab3d7bf7e306fee*

Begovic, M. M., Djuric, P. M., Dunlap, S. & Phadke, A. G. (1993). Frequency tracking in power networks in the presence of harmonics, *IEEE Transactions on Power Delivery* 8: 480–486.

Boldea, I. (2006). *Synchronous Generators*, CRC Press, Boca Raton. ISBN: 084935725X.

Concordia, C., Fink, L. H. & Poullikkas, G. (1995). Load shedding on an isolated system, *IEEE Transactions on Power Systems* 10(3): 1467–1472.

Dash, P. K., Padhan, A. K. & Panda, G. (1999). Frequency estimation of distorted power system signals using extended complex Kalman filter, *IEEE Transactions on Power Delivery* 14(3): 761–766.

Dash, P. K., Swain, D. P., Routray, A. & Liew, A. C. (1997). An adaptive neural network approach for the estimation of power system frequency, *Electric Power Systems Research* 41: 203–210.

EEUG (1987). *Alternative Transients Program Rule Book*, LEC.

El-Naggar, K. M. & Youssed, H. K. M. (2000). A genetic based algorithm for frequency-relaying applications, *Electric Power Systems Research* 55: 173–178.

Farhang-Boroujeny, B. (1999). *Adaptive Filters:Theory and Applications*, John Wiley & Sons, Inc.

Girgis, A. A. & Ham, F. M. (1982). A new FFT-based digital frequency relay for load shedding, *IEEE Transactions on Power Apparatus and Systems* PAS-101(2): 433–439.

Haykin, S. (2001). *Adaptive Filter Theory*, 4 edn, Prentice Hall, New Jersey.

IEEE Std C37.106 (2004). IEEE guide for abnormal frequency protection for power generating plants.

Karimi-Ghartemani, M., Karimi, H. & Bakhshai, A. R. (2009). A filtering technique for three-phase power systems, *IEEE Transactions on Instrumentation and Measurement* 58(2): 389–396.

Kundur, P. (1994). *Power system stability and control*, The EPRI power system engineering series, McGraw-Hill, New York. ISBN: 007035958X.

Kusljevic, M. D., Tomic, J. J. & Jovanovic, L. D. (2010). Frequency estimation of three-phase power system using weighted-least-square algorithm and adaptive fir filtering, *IEEE Transactions on Instrumentation and Measurement* 59(2): 322–329.

Kwong, R. H. & Johnston, E. W. (1992). A variable step size LMS algorithm, *IEEE Transactions on Signal Processing* 40: 1633–1642.

Lee, D. C. (ed.) (1992). *IEEE Recommended Practice for Excitation System Models for Power System Stability Studies (IEEE Std 421.5-1992)*, Energy Development and Power Generating Committee of the Power Engineering Society.

Leung, J. S. K., Hill, D. J. & Ni, Y. (2005). Global power system control using generator excitation, PSS, FACTS devices and capacitor switching, *Electric Power Systems Research* 27(5–6): 448–464.

Mojiri, M., Yazdani, D. & Bakhshai, A. (2010). Robust adaptive frequency estimation of three-phase power systems, *IEEE Transactions on Instrumentation and Measurement* 59(7): 1793–1802.

Mukherjee, V. & Ghoshal, S. (2007). Intelligent particle swarm optimized fuzzy PID controller for AVR system, *Electric Power Systems Research* 77(12): 1689–1698.

Phadke, A. G., Thorp, J. S. & Adamiak, M. G. (1983). A new measurement technique for tracking voltage phasors, local system frequency, and rate of change of frequency, *IEEE Transactions on Power Apparatus and Systems* PAS-102(5): 1025–1038.

Pradhan, A. K., Routray, A. & Basak, A. (2005). Power system frequency estimation using least mean square technique, *IEEE Transactions on Power Delivery* 20(3): 1812–1816.

Rawat, T. K. & Parthasarathy, H. (2009). A continuous-time least mean-phase adaptive filter for power system frequency estimation, *International Journal of Electrical Power & Energy Systems* 31: 111–115.

Sachdev, M. S. & Giray, M. M. (1985). A least error squares technique for determining power system frequency, *IEEE Transactions on Power Apparatus and Systems* PAS-104(2): 437–444.

Widrow, B., McCool, J. & Ball, M. (1975). The complex lms algorithm, *Proceedings of the IEEE* 63: 719–720.

Wies, R. W., Pierre, J. W. & Trudnowski, D. J. (2004). Use of least mean squares (lms) adaptive filtering technique for estimating low-frequency electromechanical modes in power systems, *Power Engineering Society General Meeting*, Vol. 2, pp. 1863–1870.

Adaptive Filtering Applications

Edited by Dr Lino Garcia

Adaptive filtering is useful in any application where the signals or the modeled system vary over time. The configuration of the system and, in particular, the position where the adaptive processor is placed generate different areas or application fields such as: prediction, system identification and modeling, equalization, cancellation of interference, etc. which are very important in many disciplines such as control systems, communications, signal processing, acoustics, voice, sound and image, etc. The book consists of noise and echo cancellation, medical applications, communications systems and others hardly joined by their heterogeneity. Each application is a case study with rigor that shows weakness/strength of the method used, assesses its suitability and suggests new forms and areas of use. The problems are becoming increasingly complex and applications must be adapted to solve them. The adaptive filters have proven to be useful in these environments of multiple input/output, variant-time behaviors, and long and complex transfer functions effectively, but fundamentally they still have to evolve. This book is a demonstration of this and a small illustration of everything that is to come.

INTECH
open science | open minds